20

Polymer-Bioglass Composite Coatings: A Promising Alternative for Advanced Biomedical Implants

Floroian Laura, Popescu Andrei,
Serban Natalia and Mihailescu Ion N.
Transilvania University of Brasov /
National Institute for Lasers, Plasma and Radiation Physics
Romania

1. Introduction

Human bone can easily regenerate in normal conditions, so in case of fractures some support devices are used to take the load from the new forming bone. However, in case of diseases, ageing and large traumas, the bone has to be helped to regenerate. Usually, large bone defects are filled with natural material from a donor site from the same patient (''autografting"). Unfortunately the transplantable bone is limited and the procedure requires the extension of the operating site (Lahav et al., 2006).

The concept of an artificial device able to help human parts to regenerate or to replace entirely one of the body functions, stimulated numerous research teams around the globe to test materials and combinations of materials aiming towards the "holly grail" of biocompatibility: the biomimetism.

There are evidences that prove early tests on bone repair using metal parts, dating from antiquity (Bliquez, 1996). Up to present time, metals have been the elements of choice for manufacturing implants or prostheses in various shapes and dimensions. Tests and clinic reports have all agreed in time, that the best metal for such devices is Ti (Emsley, 2001). It is bio tolerated by the human body and it has a low density and mechanical properties that do not negatively affect the bone (Oshida, 2006).

Orthopedics as a medicine branch does not consider bio tolerated devices as satisfactory. The general aim of an orthopedic device is to stimulate the bone to regenerate, in other words it has to be bioactive. Ceramic materials made of calcium phosphates (CaP) in various formulas, pure or doped have been extensively studied in literature for their resemblance to the mineral part of the bone (León & Jansen, 2010). Because ceramics brittle when submitted to high tensions, devices made completely out of these materials are not convenient. The common consensus is to use for the bulk implant metals as main components, covered by a very thin and adherent ceramic layer, thus making the surface bioactive (Park, 2008).

This chapter is dedicated to bioactive glasses (BG), "intelligent materials" superior in bioactivity to CaP, made of various metal oxide combinations. They change their composition in vivo after prolonged contact with body fluids, transforming in an equivalent of the mineral bone (Hench & Wilson, 1993).

2. Bioglasses and bioglass composite

2.1 Bioactive glasses

2.1.1 General considerations

The Bioglass® was invented by Larry Hench, Professor at the University of Florida, at the beginning of the 1970s. The 45S5 Bioglass composition in wt% as proposed by Hench was consisting of 45% SiO_2, 24.5% Na_2O, 24.5% CaO and 6% P_2O_5 (Hench et al., 1972).

The SiO_2 content was chosen after numerous tests that evidenced a radically different behavior of the BG in relation to bone, function of this parameter. When they have less 40% SiO_2 in their composition, the glasses do not interact with bone and do not form a connection with it. Between 40 and 50% SiO_2 glasses are highly reactive to aqueous medium. In the vicinity of the implant, ions dissolution and precipitation will take place, resulting in generation of a matrix of SiO_2 that sticks to the bone, serving as precipitation ground for new compounds synthesized in vitro, extremely similar to the inorganic part of the bone. Over 60% SiO_2 content, glasses behave as bioinert materials, being covered by a fibrous membrane in vivo (Greenspan, 1976; Gross, 1980).

Hench described a sequence of five reactions that result in the formation of a hydroxyl-carbonate apatite layer when BG are used in vivo: 1) Na, K, Ca ion migration in the extracellular fluids, 2) hydrolysis of Si-O-Si bonds, resulting in Si-OH generation, 3) total transformation of the initial layer in a Si-OH gel depleted of Ca and alkaline ions 4) precipitation of an amorphous CaP layer on the gel, and 5) mineralization of the CaP layer and its transformation into crystalline carbonated and doped hydroxyapatite (HA) similar to the mineral phase of vertebrate bones (Hench, 1981).

Related to their bioactivity, silicate glasses exhibit several advantages in comparison to other bioactive ceramics, e.g. sintered HA. It has been demonstrated that dissolution products from bioactive glasses upregulate the expression of genes that control osteogenesis (Xynos et al., 2000), which explains the higher rate of bone formation in comparison to other inorganic ceramics such as HA (Wheeler et al., 2001).

The all new concept of bioglasses bioactivity and the enormous possible composition tuning, stimulated research efforts to find and test new formulations, to add new elements to their structure, to produce composite materials bioglass-polymer/metal/ceramic in the search for biomimetic behavior (Sepulveda, 2001; Oki, 2004; Lao, 2009).

Even if countless variations of bioactive glasses can be found in literature, the original 45S5 composition remains one of the most active and efficient, being used as a comparison by almost all the papers referring to BG and still being commercially sold and used in implantology and prosthetics.

2.1.2 Other practical uses

BG are not only active for the osseous tissue regeneration, but also for some soft tissues development. Nanoparticles of such materials were proven to increase the secretion of vascular endothelial growth factor (VEGF) in vitro and to enhance vascularization in vivo (Day, 2004; Gorustovich, 2010; Leu, 2008).

By mixing BG with Ag or Zn ions, different research groups obtained antibacterial materials (Vitale-Brovarone, 2008; Haimi, 2009).

In drug delivery, particles of BG can dissolve in the body fluids releasing metal ions or medicines (Azevedo et al., 2008). Magnetite release from bioactive glasses for hyperthermia treatment of cancer (Bretcanu et al., 2006) or Co ions release to stop cells hypoxia (Gomez-Vega et al., 2000) have been reported.

2.2 BG composites

2.2.1 State of the art

Scaffolds for cells proliferation have two main components: a porous structure usually made of polymer, and a bioactive material, covering the scaffold, that stimulates cell differentiation and growth. This is the main use of BG in conjunction with polymers and reports in literature have shown excellent results in terms of efficiency. Other uses of BG-polymer mix as bone filler highly malleable composite materials, or bioactive, anticorrosive thin films for prostheses coating have been reported in literature.

As filler material for bone defects and cavities treatment, BG lack cohesiveness in bulk. Chan et al (Chan et al., 2002) showed that the addition of medium molecular weight dextran improves the malleability of the ceramic. For bioactivity comparison, they filled standardized bony defects in the lateral femoral condyles of adult New Zealand rabbits with autogenous bone, Bioglass particulates, a mixture of Bioglass® and autogenous bone and Bioglass®-dextran composite.

Postoperative healing was observed after periods of 2 days, 1, 2, 3, 6 and 12 weeks. Histologically, Bioglass® mixed with dextran produced a response essentially similar to that of Bioglass® alone. Dextran produced no adverse tissue reaction and results indicated that it was removed from the site within the first week after implantation.

Verrier et al (Verrier et al., 2004) studied biodegradable PDLLA (poly(dl-lactic acid)) /Bioglass® composites for soft-tissue and hard-tissue scaffolds. In vitro tests using A549, a human epithelial-like lung carcinoma cell line and MG63, human osteosarcoma cells, proved a strong connection between the Bioglass® content in these composites and the cells response. The authors observed 100% MG63 cell adhesion (relative to plastic control) on pure PDLLA scaffolds (0% Bioglass®) and on PDLLA composite scaffolds containing 5 wt% Bioglass®, while a 20% increase in cell adhesion was obtained on composites with 40 wt% Bioglass®. The A549 adhered 100% only on substrates containing 40 wt% Bioglass®. However, in terms of cell proliferation, after 4 weeks, A549 cells developed two times faster on PDLLA foams containing 5 wt% Bioglass® when compared to the proliferation on foams with 40 wt% Bioglass®.

Misra et al (Misra et al., 2010a) tested as scaffold for cells growth, a composite made of poly(3-hydroxybutyrate) (P(3HB)) foams of highly interconnected porosity (85% porosity) and 45S5 Bioglass® particles, introduced in the scaffold microstructure, both in micrometer and nanometer sizes (~10% bioglass content). In vitro, on cultures of MG63 osteoblast like cells, a comparison between scaffolds of P(3HB) and P(3HB)/Bioglass® evidenced a higher proliferation (by 13%) in favor of the simple polymer scaffold. However, the P(3HB)/Bioglass® composite scaffolds are not to be disregarded due to an amazing antibacterial effect verified on S. Aureus. The S. Aureus drastic reduction in the presence of composite scaffolds in vitro was explained by the pH change around the implant. The optimum living medium for bacteria colonies was of pH 7, while around the scaffold, it went up to 10 in 48 h. The composite foams were further on implanted in rats and proved to be non-toxic after one week of implantation.

The same team added multiwall carbon nanotubes (MWCNTs) to the optimal P(3HB)/ bioglass composition (Misra et al., 2010b). They proved that in vitro MWCNTs (2 wt%) improved the MG63 cell attachment and proliferation. However, by increasing the nanotubes concentration to 4-7% had negative influence on the cells development. By electrical I-V analysis in SBF, the samples with 2% nanotubes were shown to facilitate the

production of natural apatite (the signal decreased due to the isolating nature of the newly formed ceramic layer).
Yao et al. (Yao et al., 2005) synthesized poly (lactic-co-glycolic acid) (PLGA) and PLGA/BG (30% content) microparticles by an emulsification technique. When immersed in SBF for two weeks, the composite particles were covered in their entirety by a CaP rich layer. On porous scaffolds made of simple PLGA and composite PLGA/BG microparticles, rat mesenchimal stem cells were seeded in vitro. The alkaline phosphatase activity (indicative of new bone formation) was monitored and found to be ten times higher in case of the CaP covered scaffolds. The 3D porous PLGA-30% BG composites demonstrated significant potential as a bone replacement material, both supporting cell growth and promoting differentiation of marrow stromal cells to osteoblast cells.
Zhang et al. (Zhang et al., 2004) prepared by phase separation, porous (pores>100 μm) poly(l-lactide)(PLLA)/BG (average particle size: 1.5 μm) composites. A silane pretreatment of the glass resulted in better glass incorporation in the polymer matrix. The higher the glass content, the higher was the elastic modulus of the composites, but their tensile strength and break strain decreased. Glass pretreatment with silane prevented however the decrease in tensile strength with the increase of the glass content. Composites soaked in simulated body fluid (SBF) at body temperature formed bone-like apatite inside and on their surfaces. The lower the BG content, the faster was the apatite generation on the composite surface. After 1 week composites containing 9% bioglass were entirely covered by apatite, while no apatite was formed on composites with 29% bioglass. The silane pretreatment of glass particles delayed the in vitro apatite formation due to the superior incorporation of the glass in the polymer matrix and to the fewer exposed sites to SBF.

2.2.2 Synthesis of bioglass composite nanostructures

There are a few methods allowing in situ synthesis of BG and their mix with other compounds on site. Each technique has its own advantages and the type of application should recommend the use of a specific method, depending on the foreseen final results: high synthesis efficiency for mass production, high purity of final products at lower rates and/or unusual shape of BG nanostructures for new applications (Boccaccini et al., 2010).
SOL-GEL The method is largely used to obtain nanoparticles of numerous metallic and oxidic materials by precipitation following chemical reactions in liquid medium. BG in the system $CaO–P_2O_5–SiO_2$ in nanometric structures have been synthesized by sol-gel for antibacterial applications in combination with Ag, or for scaffolds coating on HA porous structures (Chen, 2009; Esfahani, 2008).
The major advantage of the sol-gel technique is its versatility. The morphology and size of BG nanoparticles could be tailored by varying the synthesis conditions and the feeding ratio of reagents (Couto, 2009; Hong, 2009).
However, sol-gel can be a time consuming process, due to the necessity of additional steps. Usually, the obtained nanostructures have to be exposed to heat-treatment in order to remove organic additives. It is also a method limited in terms of compositions that can be produced. Because of the numerous steps involved, batch-to-batch variations in terms of compositions are highly possible.
FLAME SPRAY SYNTHESIS The metalorganic deposition uses metal–organic precursor compounds to produce nanoparticles at temperatures above 1000 ^{0}C. The flame spray synthesis, a derivative of this technique, starts from a liquid compound that is pushed by a high flux of oxygen through a nozzle, forming a spray which is ignited. As the spray is

burning, the organic constituents of the liquid precursor completely burn, decomposing in H_2O and CO_2, and metal constituents oxidize to form the nanoparticles. Consequently, the process allows the production of any kind of nanoparticulate mixed-oxides with high chemical homogeneity. By using flame spray synthesis, therefore, the preparation of nanoparticles of different BG compositions has become possible.

Mixtures of 2-ethylhexanoic acid salts of calcium and sodium, hexamethyldisiloxane, tributyl phosphate and fluorobenzene were used for BG nanoparticles synthesis (Brunner et al., 2006). The primary particles produced are usually spherically shaped with different degrees of agglomeration.

LASER SPINNING The team of Quintero et al used the laser spinning technique to obtain glass fibers with diameters in the nanometer to micrometer scale (Quintero et al., 2007a).

Large quantities of nanofibres can be produced with good control over chemical compositions and without the necessity of any chemical additives or post heat treatments. The process is very fast; nanofibres being produced in several microseconds. It involves the quick heating and melting of a small amount of the precursor material up to high temperatures using a high power laser. At the same time, a supersonic gas jet is injected into the melt volume to blow the molten material (Quintero, 2007a, 2007b, 2009a). The molten material is quickly spread and cooled by the supersonic gas jet (Quintero et al., 2009a). Long fibers with large length to diameter ratios can be produced by the elongation of the viscous molten material. The obtained BG is amorphous because of the high cooling speed.

Quintero et al. (Quintero et al., 2009b) developed 45S5 and 52S4.6 BG nanofibers and investigated the possibility of using these nanofibers as scaffolds or as reinforcement in polymeric matrix composites. Bioactivity test results were promising, the fibers forming very fast apatite coatings when immersed in SBF.

PULSED LASER TEHNOLOGIES Pulsed laser technologies emerged in late ’80 of the last century as a major alternative for ablation and deposition of stoichiometric compounds in form of nanoparticles, nanofibres and nanostructured thin films. In pulsed laser depositions (PLD) the substance is expulsed from target under the action of pulse laser radiation and transferred to a nearby substrate. PLD presents numerous advantages in respect with other deposition technique among which we mention: accurate control of the stoichiometry of the deposited material; reduced film contamination due to the use of laser light; promotion of the growth of crystalline structures for desired applications; energy source independent of the deposition environment; relative simplicity of the growth facility offering great experimental versatility (multilayers, doping); control of the film thickness (with a precision of > 10^{-2} Å/pulse).

PLD was applied to the synthesis of BG nanoparticules and their deposition well- separated or assembled in these films (Floroian, 2008, 2010). These structures were converted in bioapatite after prolonged immersion in SBF.

However, PLD failed when extended to composite polymer - bioactive glass (**PBG**) transfer and deposition. The polymer was irreversibly photochemically decomposed and damaged under direct action of intense UV laser pulses (Pique, 2007). The only solution was conferred by another pulse laser deposition technology – the matrix assisted pulse laser evaporation (MAPLE).

We will review in the next sections recent results obtained in MAPLE deposition of polymer (polymethyl methacrylate, PMMA) in form of nanoparticle thin films.

3. MAPLE for thin films synthesis and deposition

3.1 MAPLE: definition and working procedure

The deposition of polymer, biopolymer and protein materials needs a special protection, which could be provided by MAPLE. Basically, the difference between PLD and MAPLE is target preparation and laser target interaction.

Specific to MAPLE is the use of a composite cryogenic target consisting of a mixture of the organic active material dissolved in a volatile solvent. The solvent must be carefully selected so that it absorbs majority the UV radiation. It has to present a high freezing point and the organic/polymeric material must to present a high solubility in solvent to be deposited (Cristescu et al., 2006). No chemical reaction is permitted between solute (organic polymer) and solvent. Two processes develop under the action of incident laser pulse: the frozen target is evaporated and the organic material is released. The organic molecules reach sufficient kinetic energy by collective collisions with the evaporating solvent molecules to be transferred in gas phase to the collecting substrate (Mihailescu et al., 2010). Finally, the volatile solvent is gradually evacuated by the vacuum system during the deposition of the solute on the substrate in form of thin film. A schematic representation of the MAPLE process is given in Fig. 1.

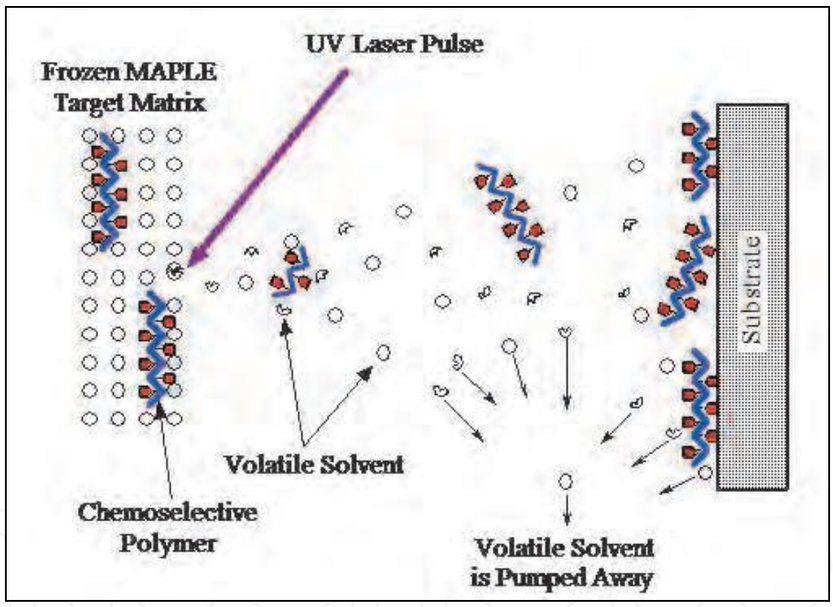

Fig. 1. Schematic of the MAPLE evaporation process (Mihailescu et al., 2010)

3.2 MAPLE experiment

To types of bioglasses were used for deposition: BG57 whit the composition 56.5% SiO_2, 11% Na_2O, 3% K_2O, 15% CaO, 8.5% MgO, 6% P_2O_5 and BG61 having the composition 61.1% SiO_2, 10.3% Na_2O, 2.8% K_2O, 12.6% CaO, 7.2% MgO, 6% P_2O_5 (Veljovic et al., 2009). Biomedical grade 4 Ti was used as substrate because it exhibits a good biocompatibility and is resistant to corrosion, properties which make it a good candidate for fabrication in orthopedic implants. The composite consisted of BG powder mixed with PMMA grains and the mixture was dissolved in chloroform (matrix material). The target was prepared from 0.5 g PMMA dissolved in 19.3 ml chloroform with addition of 0.08 g of either BG57 or BG61. The obtained

suspension was frozen at liquid nitrogen temperature and kept during experiments at low temperature using a cooling device (cooler).
A KrF* excimer laser source (model COMPexPro from Coherent) (λ =248 nm, τ_{FWHM} =25 ns) was used for target evaporation. The depositions were conducted in a stainless steel chamber which was first evacuated down to residual pressure of 10^{-4} Pa (Fig. 2).

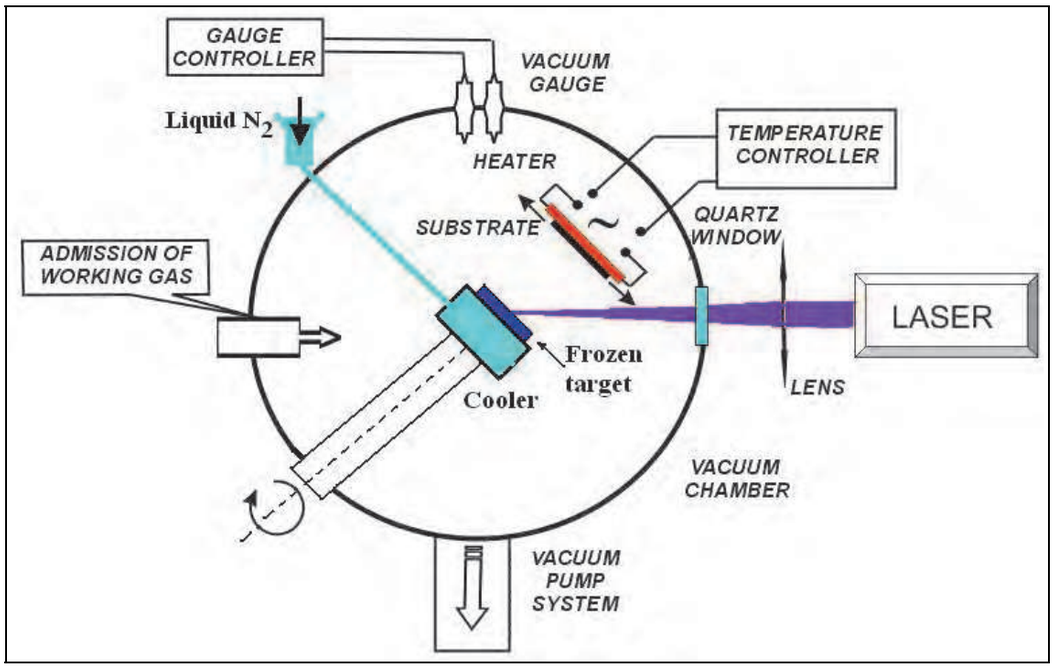

Fig. 2. MAPLE experimental device (Mihailescu et al., 2010)

The dynamic pressure inside chamber during deposition was maintained at 2.7 Pa. The laser beam was incident at 45° on target's surface. The expulsed material was collected onto the Ti substrates placed parallel to the target at a separation distance of 3 cm. Before the deposition the chemically etched Ti (5 mm diameter and 0.5 mm thick) substrates were carefully cleaned with deionized water in a TRANSONIC T 310 ultrasonic bath. The fluence was set for each deposition at 0.55 J/cm² and the irradiation spot was of 16 mm² area.
In order to improve films adherence, during the depositions the substrate was moderately heated at 35 °C. For the deposition of each film, 5000 subsequent laser pulses have been applied.
During the film growth, the target was continuously rotated at 0.3 Hz and translated along two orthogonal axes in order to avoid drilling and to ensure a uniform deposition.

3.3 Post deposition investigations

3.3.1 Morphological and structural characterization

The PBG deposited structures were characterized by Fourier transform infrared spectrometry (FTIR), energy dispersive X-ray spectroscopy (EDS), atomic force microscopy (AFM), scanning electron microscopy (SEM) and confocal scanning laser microscopy (CLSM).
FTIR analyses were performed using a Nicolet 380 apparatus. The spectra were taken in the absorbance mode. EDS cartography and SEM images were recorded with a Hitachi S2600N

microscope. AFM investigations were carried out in a semi-contact mode with AFM NTEGRA Vita equipment.
For nondestructive investigation of specimens by CLSM, a Leica TCS SP system was used, equipped with a He-Ne laser emitting at 633 nm wavelength and a set of PL Fluotar (40X magnification, 0.7 numerical aperture) objectives. The images were obtained in reflection mode. Data processing and displaying were made by Leica software.

3.3.2 Biocompatibility and bioactivity evaluation

To test the nanomaterials biocompatibility and bioactivity we evaluated the cells adhesion, the cellular viability, cellular proliferation and the capacity of the films to form a biological active layer of apatite (BHA) on surface.
For this purpose human osteoblast cells were harvested then maintained in a McCoy's culture medium supplemented with 10% inactivated bovine fetal serum, 50 U/ml penicillin, 50 mg/ml streptomycin and 1% L-glutamine. The cells were split every 2 days by a ratio of 1:3 and incubated at 37 °C in 5% CO_2. All studies were done 72 hours after cell cultivation on the studied films using FACS Calibur flow cytometer (BD Biosciences) and Leica TCS SP system in fluorescence mode.
The bioactivity of the films was assessed in vitro by soaking the composite films into simulated body fluid (SBF) followed by FTIR spectroscopic and CLSM analyses to determine the extent of BHA formation on surface.

3.3.3 Electrochemical measurement

The samples were immersed in SBF for 7, 14, 28, 35 or 42 days and the potentiodynamic measurements were performed with Palm Sens potentiostat (Palm Instrument) having three electrodes configuration with an Ag/AgCl reference electrode and a platinum wire as the counter electrode. As the working electrodes small discs of bare Ti or Ti substrates coated with nanocomposite films were used. In order to warrant reliable results, the potentiodynamic polarization measurements were repeated three times in SBF in each case.
The curves were recorded when scanning the working potential from (-1 to +2 V) with a scan rate of 0.002 V/s. The electrochemical impedance (EIS) measurements were carried out in an electrochemical cell with a PC-controlled Autolab frequency response analyzer using FRA 4.9 software (Autolab PGSTAT 100 Eco Chemie). A sinusoidal voltage perturbation of amplitude 0.01 V was applied, scanning from 10,000 Hz to 0.1 Hz with 10 points per frequency decade (auto-integration time 5 s).
The fitting to electrical equivalent circuits was performed with the FRA 4.9 software.

4. Polymer (PMMA) - bioglass thin films obtain by maple: physical, chemical and biological characterization

4.1 Chemical characterization: structure and composition

The chemical composition of PBG thin films was investigated by different techniques: FTIR, EDS and XPS. FTIR analyses revealed identical molecular bindings in powder and obtained films and the absence of any other peaks due to impurities (Fig. 3). These features make a strong case for MAPLE preservation of the chemical composition of the base material after transfer.
PBG structure depends on the wt ratio between P and BG. Thus for a ratio larger than 7.5 the polymer peaks prevail, while for a ratio inferior to 7.5 are higher BG peaks (Fig. 3).

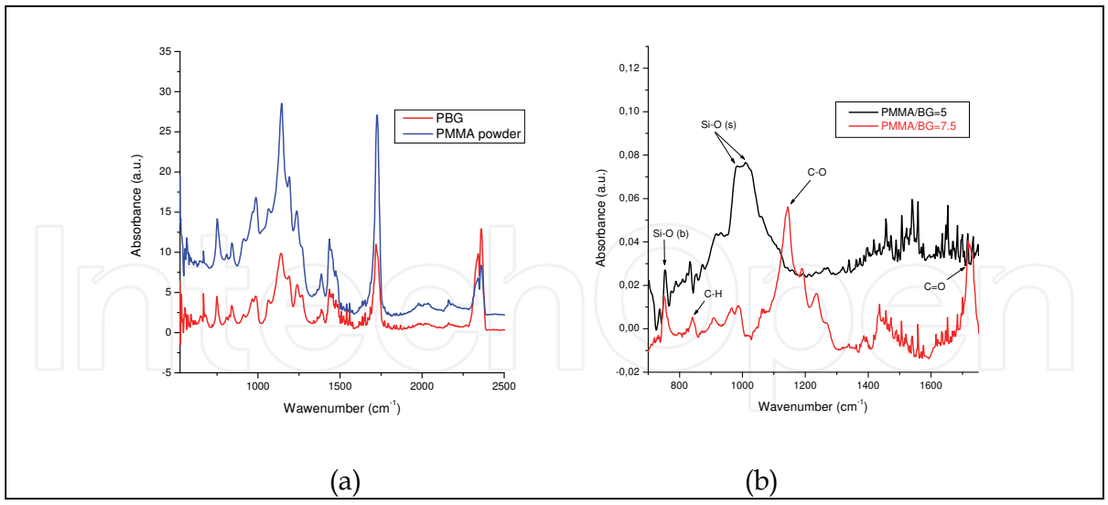

Fig. 3. Main vibration bands present in the FTIR spectra of PBG coatings obtained by MAPLE depending on PMMA/BG wt ratio

The EDS cartography of the PBG coating (Fig. 4) shows that all bioactive glass elements have been preserved in deposited nanostructures and were homogeneously spread over the whole investigated area.

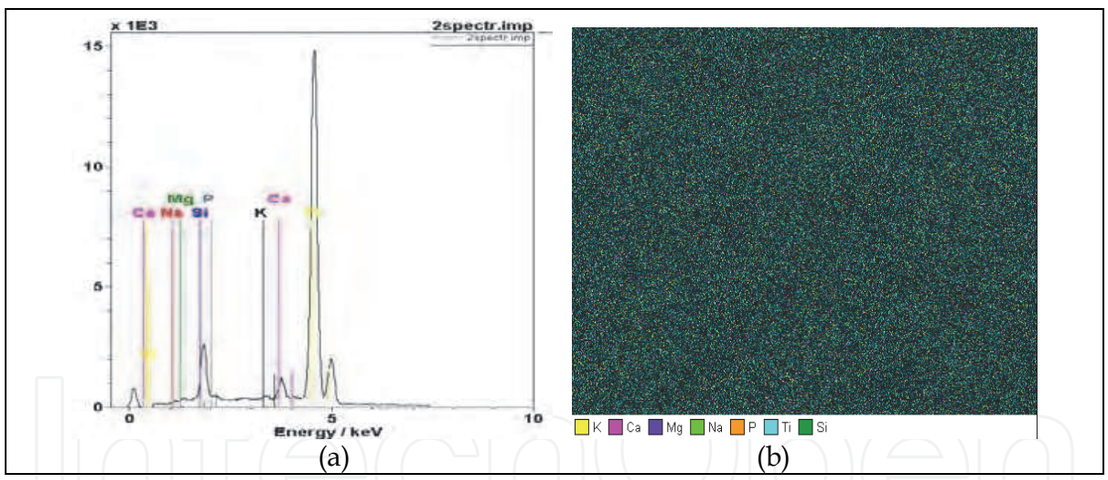

Fig. 4. EDS spectrum (a) and EDS cartography (b) of a PBG film deposited by MAPLE

FTIR and EDS analyses were performed on a large number of samples, and the similar results obtained point to the reproducibility of the method also confirming the stoichiometric transfer of material by MAPLE.

4.1.1 Morphological investigations

The morphology of PBG coatings was investigated by SEM, AFM and CLSM. We observed by SEM (Fig. 5 a, b) that PBG structures are rather uniform and compact.
They consist of droplets of variable size, characteristic to MAPLE or PLD depositions (Gyorgy, 2007; Tanaskovic, 2007, 2008).

The droplets are in the micrometric range, and are randomly spread across the surface. These features are considered favorable (Nelea et al., 2004) to the growth and proliferation of cells which can easily and deeper infiltrate their pseudopodia into surface imperfections and pores. These observations were supported by AFM evidence in 2D and 3D images respectively (Fig. 6 a, b).

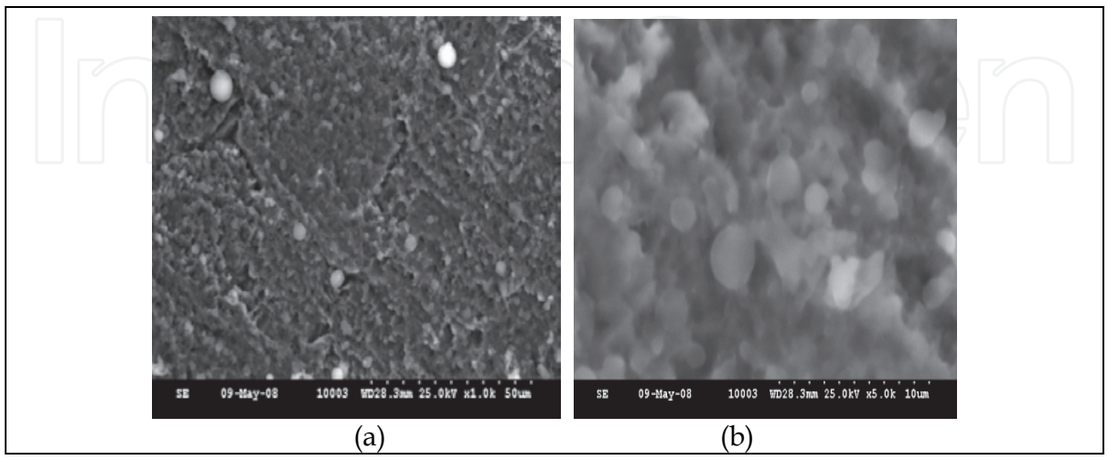

Fig. 5. SEM micrographs showing a typical surface morphology of a PBG coating: (a) general view; (b) detail from (a)

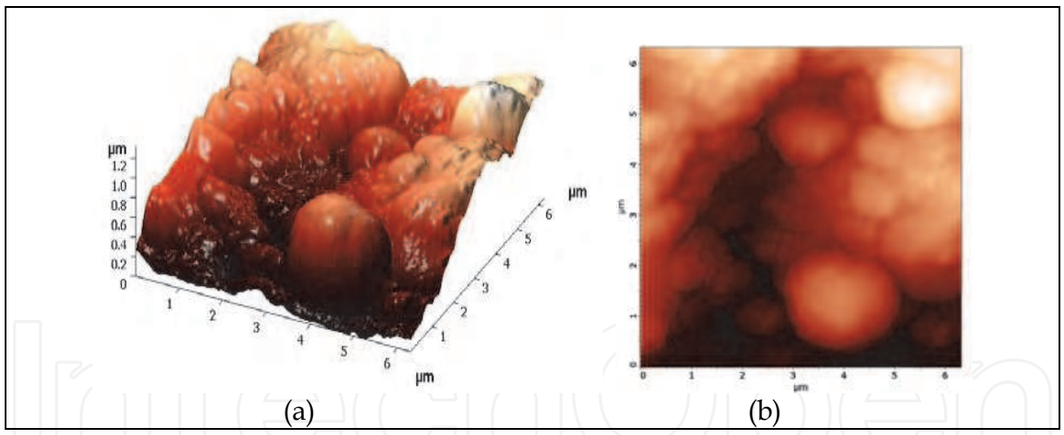

Fig. 6. 3D (a), 2D (b) typical AFM images recorded in case of PBG coating.

The confocal microscopy study also shows a uniform topography of PBG coatings (Fig. 7).
3D images of the deposited PBG thin films (Fig. 8 a, b) revealed the formation of a structure with a characteristic configuration, consisting of a great number of protuberances with few micrometers maximum height. Such features favor biocompatibility because it involves a significant increase of specific area of the deposited biofilms and the proliferation of viable cells (Nelea, 2004).
All these aspects are confirmed by the images below (see Fig. 9), which show the film surface profile compared with the profile of titanium substrate. Initial titanium surface profile shows that this area has a lot of scratches, thin grooves 1-2 µm wide, some reaching up to 13-14 µm deep and some small, with depth less than 1 µm, because titanium substrate

was polished and chemically etched to increase the active surface. This titanium area is ideal for implants: it has a suitable morphology for good cell adhesion and growth of bone and an appropriate roughness for increasing of bone-implant interaction activity.
After PBG thin film deposition all irregularities become lower, having 0.2-5 μm depth but the surface remains rough "friendly" for applications in the field of implantology.

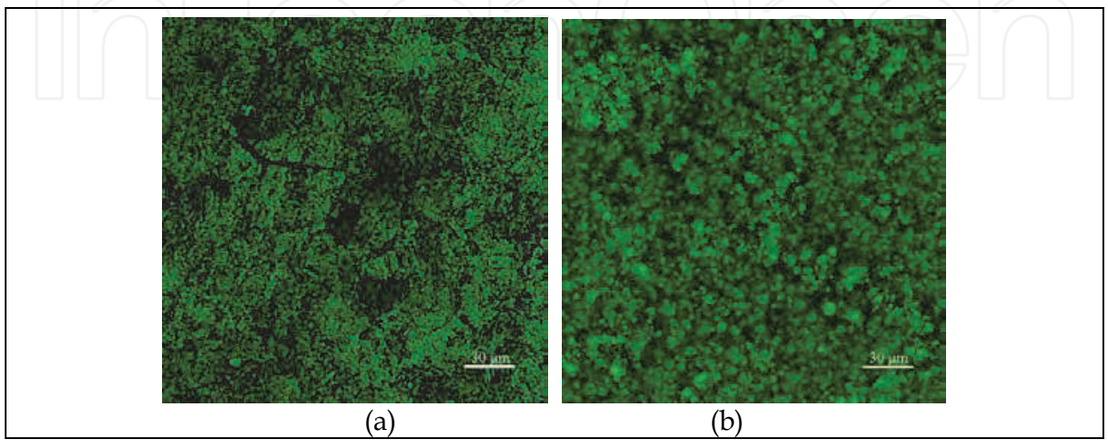

Fig. 7. Topography (40X magnification, 0.7 aperture, zoom 1) for: a) titanium substrate, b) PBG film

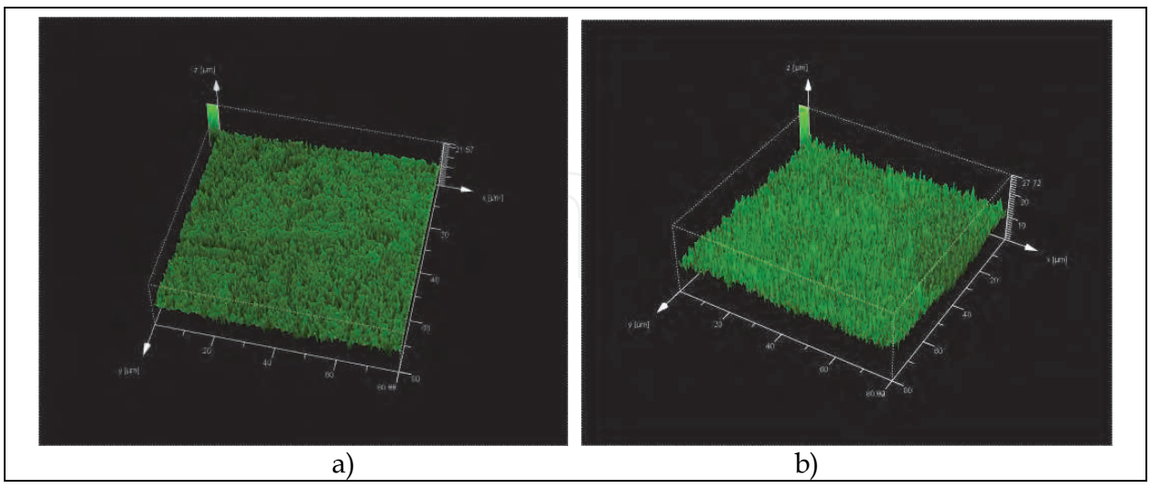

Fig. 8. 3D images (40X magnification, 0.7 aperture, 3.12 zoom) for: a) titanium substrate, b) PBG film

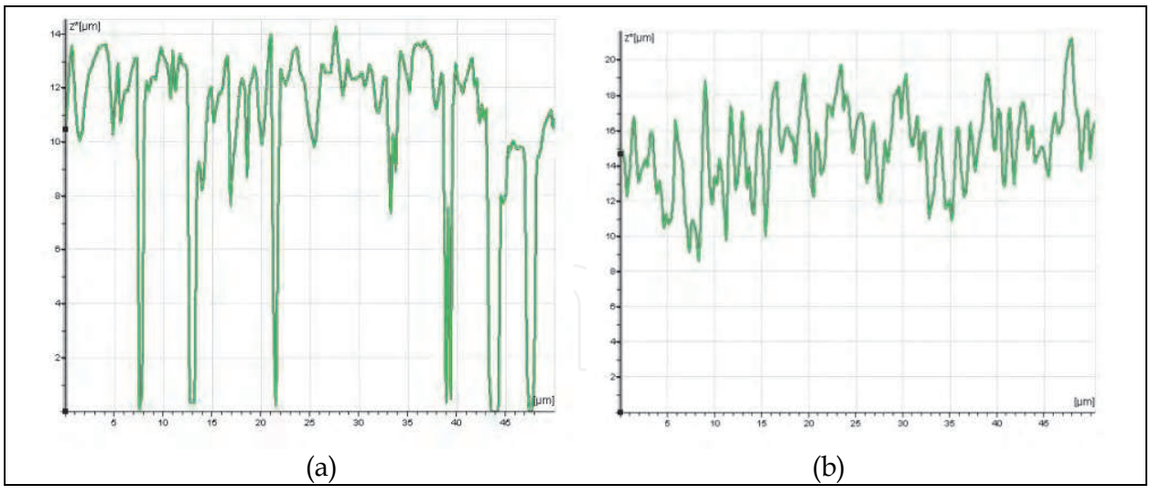

Fig. 9. Surface profiles along a random 50 µm length zone in case of (a) titanium substrate and (b) PBG films, made with a CLSM microscope, 40X magnification, 0.7 aperture, 3.12 zoom

4.1.2 Evaluation of film - substrate adherence

To estimate the adherence of PBG films to metallic substrate we applied scratch-test method to thin films of identical thickness of two types of BG (57 and 61) and two types of PBG nanostructures (with 57 and 61 bioactive glass). The critical loads for the PBG samples have similar values (see tab. 1), with a little higher value in case of PBG61, which shows that this film is more resistant to mechanical stress. The critical load values of PBG films are with an order of magnitude lower than for pure glass films because PMMA is much softer than glass. The critical load for more rough samples is bigger, pointing to a better adhesion to substrate. Despite the high roughness, the results are very repeatable as they show the low value of standard deviation.

Lc (N)	BG57	BG61	PBG57	PBG61
Data 1	0.55	0.82	0.036	0.048
Data 2	0.68	0.67	0.032	0.052
Data 3	0.63	0.61	0.028	0.056
Media	0.62	0.70	0.032	0.052
Standard dev.	0.11	0.12	0.004	0.004

Table 1. Critical load values of BG and PBG structures deposited on Ti substrate.

All peculiarities evidenced by the physical-chemical investigation of PBG coatings were similar for nanostructures contain BG57 or BG61 glass. This sustains the assertion that the two coatings are identical from the point of view of their physical-chemical parameters.

4.2 Biocompatibility and bioactivity assay

4.2.1 In vitro biotests

The osteoblast cells cultivated on PBG surface showed a good viability (Fig. 10), greater even than in the control experiment performed on a borosilicate glass: 85.92% viable cells on PBG surface versus 81.03% viable cells on control surface, the number of events recorded being statistically relevant.

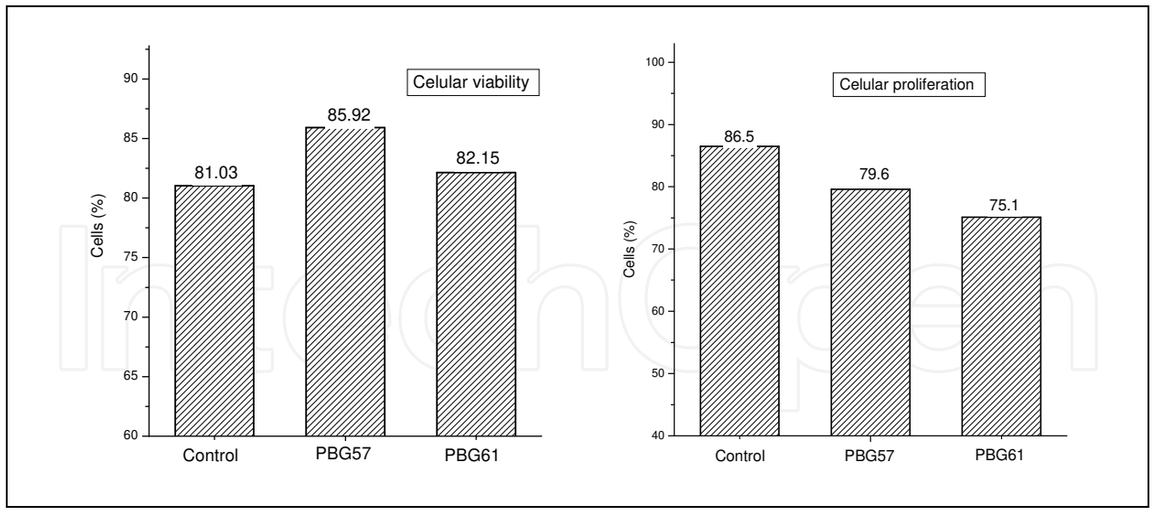

Fig. 10. Viability and proliferation at 72 hours after cell cultivation on control surface and on MAPLE deposited structures

The proliferation experiments were also performed by flow citometry. The primary osteoblasts were scored on day 0 with carboxifluorescein diacetat (CFDA), which has the ability to freely diffuse into cells. It becomes fluorescent when the acetate groups are cleaved by intracellular esterase, which gives rise to a fluorescent CFSE (carboxifluorescein succinimil ester) compound that emits in green at 517 nm. The succinimil ester groups react with the intracellular amines, forming fluorescent conjugates that are retained in the cells. Following division, the daughter cells inherit half of the fluorescence precursor cells, each generation being highlighted as a peak in FACS histogram. The osteoblast cells cultivated on the PBG surface proliferate extensively (see fig. 11), all these results showing a very good surface reaction from the cells.

The cellular adhesion is one of the essential initial events for the cell proliferation and the subsequent differentiation of the bone before the formation of the bone tissue. The analysis of the cellular distribution of the cytoskeleton proteins (vinculina) that mediate the interactions between the actin filaments and integrin (specific receptors of adhesion plaques) can provide useful information regarding the degree of contact between osteoblasts and the nanostructured films.

The samples were washed with phosphate buffer saline, fixed with 4% paraformaldehyde, and permeabilised with 0.2% Triton X-100 for 3 min. The actin filaments were labeled with Alexa Fluor 594 phalloidin (Invitrogen) and vinculina with anti-vinculina antibody (mouse monoclonal from Sigma) followed by Alexa Flour 488 goat anti-mouse antibody (Invitrogen). The primary osteoblasts grown on PBG structure were visualized with a fluorescence microscope (Fig.11). The staining of the two proteins of interest was made with fluorescent marks visualized on the green channel for vinculina and respective red channel for actin. The cells' nuclei were stained with DAPI and they were visualized on the blue channel of fluorescence. The overlap of images shows the spatial localization of vinculina and actin on the film surfaces, with some co-localization of vinculina with actin filaments ends. This suggests that vinculina was activated and was able to induce the generation of focal adhesion points.

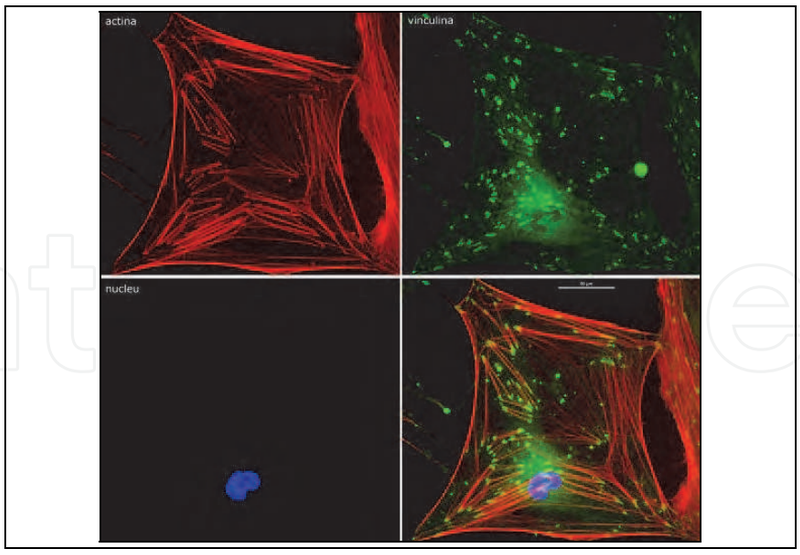

Fig. 11. Fluorescence image of PBG film surface: red staining for actin, green staining for vinculina and blue staining for nucleus, after 3 days of culture (400X) magnification

The osteoblasts are well spread out on the PBG films, with numerous contact points with the PBG surface indicating a good cell adhesion. The actin filaments are well highlighted in all cells and evidence the cytoskeleton organization. The cells present an irregular disposal due to the irregular surface of the film, with the pseudopods infiltrating into the depth of the material which increases cellular adhesion. The cells are well spread out and attached to the film on a large surface which is an evidence of the films biocompatibility. The bioactivity of the films was assessed in vitro by soaking the composite films into SBF followed by FTIR spectroscopic and CLSM analyses to determine the extent of BHA formation on surface. The SBF was prepared according to Kokubo prescription (Kokubo et al., 1990) and it has an ionic concentrate on equal to human plasma. Table 2 collects the ionic concentrations of SBF and blood plasma.

4.2.2 PBG films immersion in SBF

The titanium disks coated with the sintered films were tested by immersion into 25 ml SBF for different times then analyzed. We investigated the bioactivity for two types of PBG films obtained from targets which had a different PMMA/BG wt ratio: PMMA/BG=5 and PMMA/BG =7.5. For the first composition the target contained 0.6 g PMMA reinforced with 0.12 g BG57 bioactive glass particles dissolved in 19.3 g chloroform. For the second was used less glass, i.e. 0.08 g.

Composition (mM)	Na^+	K^+	Mg^{2+}	Ca^{2+}	Cl^-	HPO_4^{2-}	SO_4^{2-}	HCO_3^-
SBF	142	5	1.5	2.5	147.8	1	0.5	4.2
Blood plasma	142	5	1.5	2.5	103.0	1	0.5	27.0

Table 2. Comparison of ionic concentrations of SBF and blood plasma

In case of first composition, after one day of immersion into SBF solution, we can notice the growth of amplitude for all peaks (see Fig. 12 a– red plot) that indicates the forming of a rich

superficial layer, where all elements have a greater concentration. This is consistent with other experimental observations (Hench, 1991; Saiz, 1998) and it is accompanied by the loss of soluble silica into the solution, accentuated by the depreciation of the surface's quality observed by microscopically surface investigation.

After one week of immersion into SBF, major transformations were clearly noticed on the surface of the coating (see Fig. 12 a– green plot). They indicate the decrease of silica concentration and the formation of the BHA layer on surface coating. The corresponding peaks for BHA are well observed at 630, 865, 961, 1031 and 1090 cm^{-1}. They correspond to asymmetric (peaks at 1031 and 1090 cm^{-1}) and respective symmetric (peak at 961 cm^{-1}) stretching of $P-O$ bond in $(PO_4)^{3-}$, to $(HPO_4)^2$ (peak at 865 cm^{-1}) and also to the vibrational mode of OH (peak at 630 cm^{-1}). At the same time the peaks belonging to the glass disappeared.

After two weeks of immersion, only the peaks corresponding to BHA remain visible (see Fig. 12 a– blue plot). Their intensity increase in time suggesting the growth of BHA layer.

These certify two things: the dissolution of the bioactive glass and the formation on surface of a freshly growing BHA layer.

This behavior is similar to that reported for bulk glasses in the SiO_2-Na_2O-K_2O-CaO-MgO-P_2O_5 system, immersed into SBF (Gomez-Vega, 1999; Hill, 1986; Ogino, 1980; Saiz, 1998) and it is in accordance with the mechanism of apatite formation described by Hench for Bioglass® (Hench, 1991).

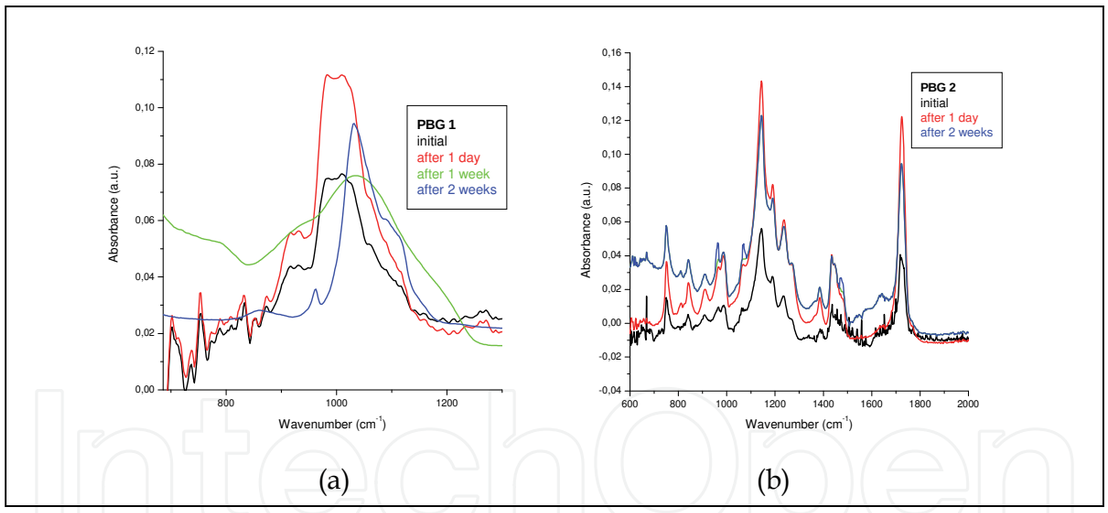

Fig. 12. FTIR spectra for different PBG compositions: PMMA/BG=5 (a) and PMMA/BG=7.5 (b) after their immersion into SBF at 37 °C

However the bioactivity of material is lower than that of pure bioactive glass BG films (Floroian, 2008, 2010) where the growing of BHA layer starts earlier, after few days of immersion. PMMA addition reduces the bone bonding ability of bioactive glasses. This is in good agreement with the studies of the effect of other materials doping in bioactive glasses published by Ohura and Anderson (Anderson, 1988; Ohura, 1982). PMMA does not dissolve into physiological fluids but remains on the metallic substrate. This way, the implant corrosion and the release of metallic ions into the body are prevented while the structure preserves the glass bioactivity. The more glass they contain, the more bioactive the layers are.

The second PBG composition showed a different behavior. No change is visible in his FTIR spectrum before two weeks of immersion (see Fig. 12 b). It presents a very low activity and the studies described below were made on films having the first composition (wt ratio PMMA/BG=5, noted PBG. 3D CLSM images for PBG thin films after 1, 7, 14 immersion days into SBF show changes in time of the surfaces morphology and of their roughness. The decrease of surface roughness within 7 days of immersion (see Table 3) suggests the attenuation of surface irregularities due to the dissolution of the glass. However, the roughness increases after 14 days of immersion that indicates the covering of surface with a thin BHA layer.

Immersion time	RMS (μm)
0 days	2,365
1 day	2,152
7 days	2,042
14 days	2,417

Table 3. Time evolution of surface roughness of PBG structures in SBF

Thus 3D images (see Fig. 13), topographical images (see Fig. 14) and surface profiles images (see Fig 15) sustain observations by FTIR .

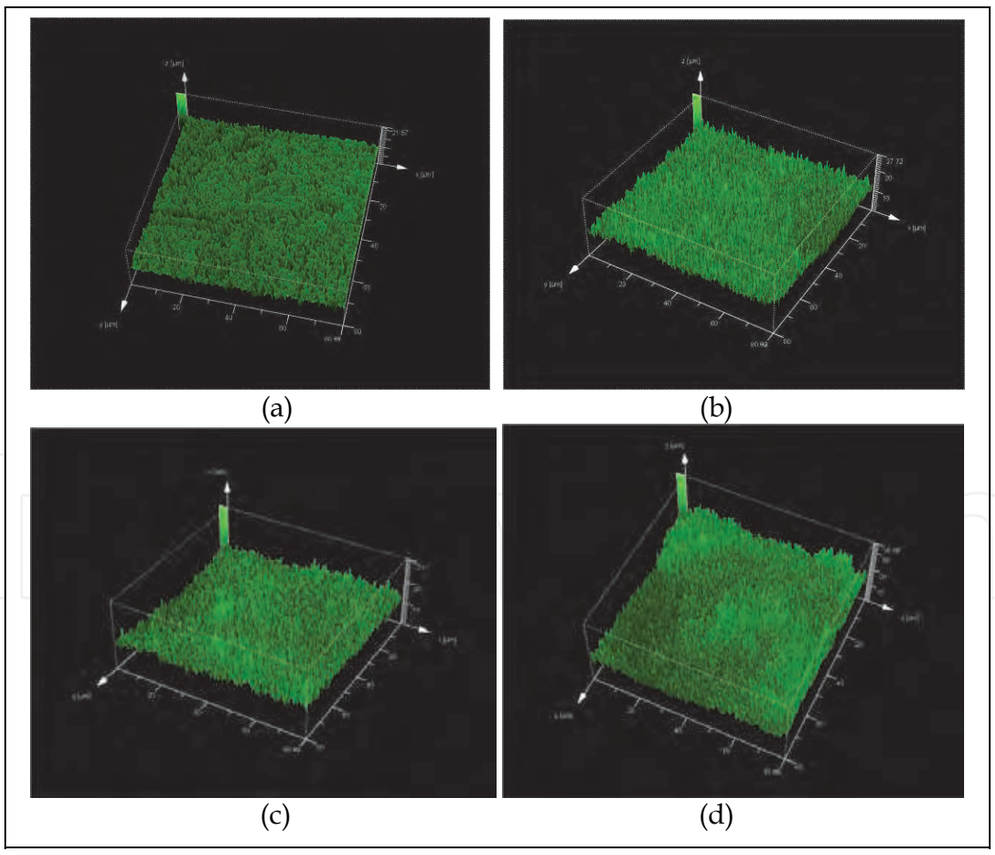

Fig. 13. 3D images (40X magnification, 0.7 aperture, 3.12 zoom) for: (a) titanium substrate, (b) PBG initial film,(c) PBG film after 1 week of immersion into SBF, (d) PBG film after 2 weeks of immersion into SBF

The CLSM analyses certify the glass dissolution and the appearance on the surface of a freshly BHA layer after two weeks of immersion into SBF. In figures 14 and 15 we can see particulates of variable size in the micrometric range that are randomly distributed over the whole investigated area. Surface root mean square roughness becomes RMS=2.417 μm.

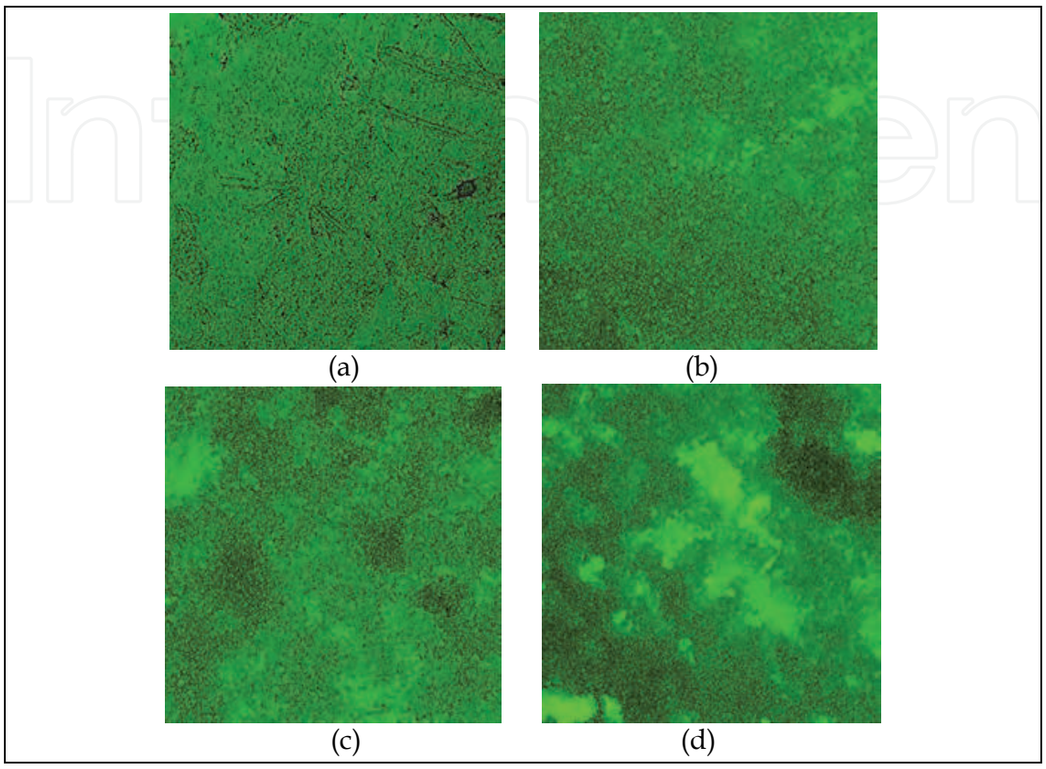

Fig. 14. Topography (40X magnification, 0.7 aperture, 1 zoom) for: titanium substrate (a) and PBG film: initially (b), after 1 week (c), and after 2 weeks of immersion into SBF (d)

4.2.3 Corrosion resistance assessment

The physiological fluids influence upon different coatings was investigated by electrochemical methods, largely spread nowadays because of their high sensibility (Karthega, 2008; Oliveira Brett, 2003).

The corrosion resistance parameters were comparatively studied by potentiodynamic polarization and electrochemical impedance spectroscopies (EIS). The electrochemical parameters of the involved processes were estimated and the electrical parameters of the circuits were verified by fitting the experimental data using equivalent electrical circuits.

Electrochemical polarization investigations were performed for bare uncovered Ti samples (Ti), samples covered with bioglass only (BG57 and BG61) or with the nanocomposite (PBG57 and PBG61). Some of samples PBG were immersed for 28 days in SBF and were covered by a BHA thin layer. The small discs of Ti, BG, PBG and BHA samples were used as working electrodes.

From the potentiodynamic polarization plots and the Tafel diagrams (Fig. 16), the corrosion parameters (the corrosion potential E_{corr}, the corrosion rate i_{corr}, the passive domain E_{pass} and the breakdown potential E_{bd}) and their average values (Table 4) have been obtained.

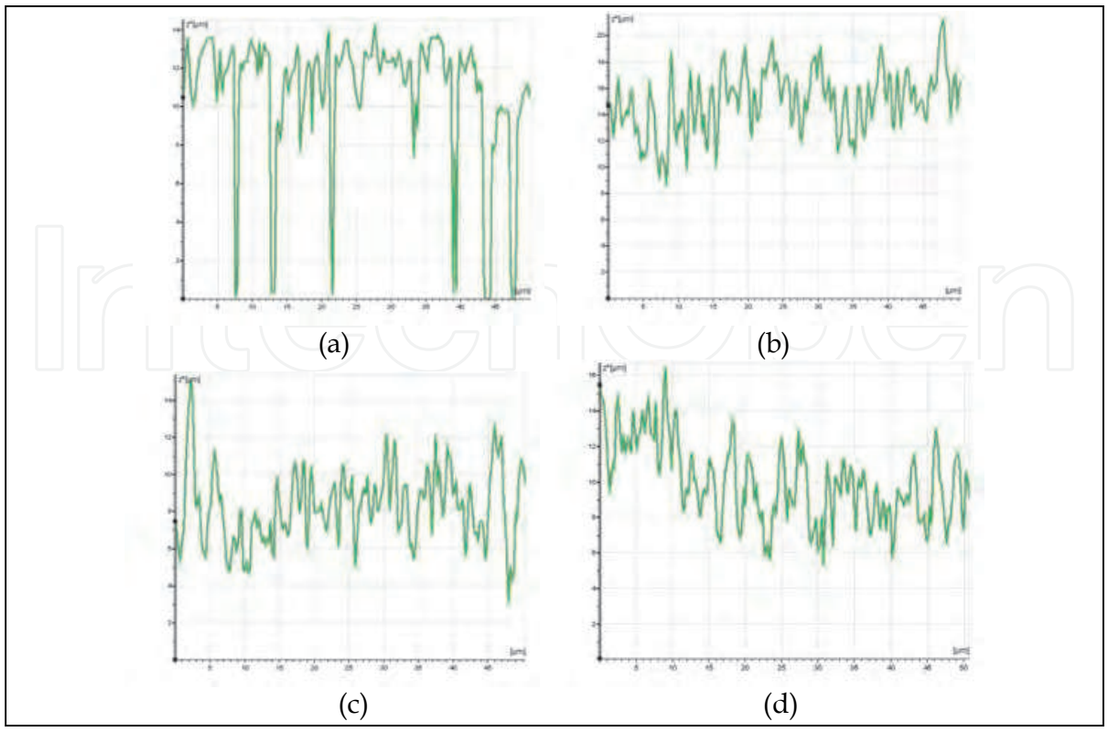

Fig. 15. Surface profiles along a random 50 µm length zone recorded with a CLSM microscope, 40X magnification, 0.7 aperture, 3.12 zoom) for: titanium substrate (a) and PBG film: initially (b), after 1 week (c), and after 2 weeks of immersion into SBF (d)

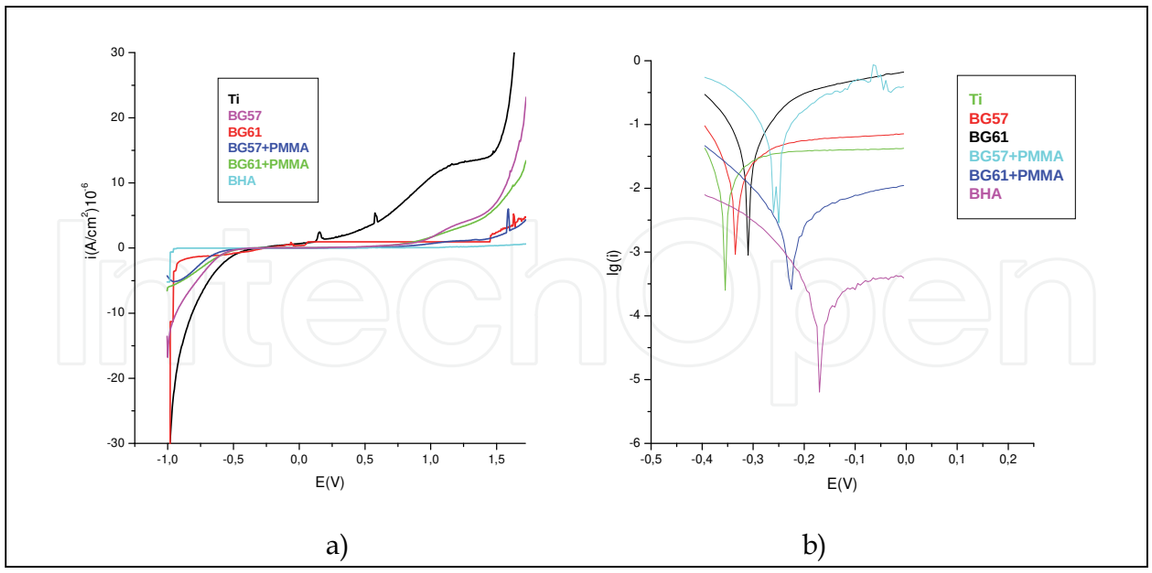

Fig. 16. Polarisation curves (a) and Tafel diagrams (b) into SBF for Ti, BGs, PBGs and BHA

The corrosion rate of uncoated Ti was i_{corr} =1.32 µA/cm². This small value justifies the preference given to Ti as compared to other metals for implants manufacturing. i_{corr} drops 2.3 times for both BG sample and 25 times for both PBG samples. This means that the

bioactive glass and especially PBG layers protect very well the Ti implant against corrosion. Further arguments in support of this behavior come from the significant increase of E_{bd} and E_{pass}.

Film	E_{cor} (mV)	i_{cor} (μA/cm²)	E_{bd} (mV)	E_{pass} (mV)
Ti	-357	1,320	141	541
BG57	-335	0,560	535	1407
PBG57	-251	0,053	733	1246
BG61	-310	0,260	671	2303
PBG61	-224	0,022	1454	1512
BHA	-166	0,025	1080	1792

Table 4. Average values of corrosion parameters for uncoated Ti (Ti), samples coated with bioglass only (BG) and composite material (PBG). Corrosion parameters are also indicated for PBG sample after 28 days of immersion in SBF (BHA).

These PBG coatings are not only efficiently isolating the metal from corrosive fluids, but also introduce a very high electrical resistance, of about $10^{10}\,\Omega$. This interposes a resistance of the order of $10^{6}\,\Omega$ between the anodic and cathodic centers on the metal surface that become really isolated from each other, so that the corrosion current density gets neglectable (Perez, 2008).

The prolonged immersion in SBF is resulting in a further enhancement of anti-corrosive action of the layers. Indeed, i_{corr} dropped 2.1 times while E_{corr}, E_{bd}, E_{pass} increased ~ 1.5 times in case of samples BHA as compared to samples PBG. One can say that according to these electrochemical measurements the PBG layer stands for the best anti-corrosion protection of Ti implant surface, especially after prolonged immersion in SBF.

The electrochemical impedance data for the PBG samples after different times of immersion in SBF at room temperature were recorded at 0.1 V and they are shown in the complex plane in figure 17. These plots aim to visualize the differences in the adsorption behavior and charge separation of the interfacial region in different experimental conditions. The fitting of spectra was done using an equivalent electrical circuit, which comprised R_S, the cell (solution) resistance, in series with a parallel R_p-CPE configuration (see Fig. 18). The constant phase element (CPE) was necessary because of the non-homogeneous surface and was modeled as a non-ideal capacitor of capacitance C and roughness factor n (n = 1 corresponds to a perfectly smooth surface). R_p stands for the charge transfer resistance. The values of R_s, R_p, CPE and n obtained based upon the model fitting, are given in Table 5. The maximum phase angle was determined in each case using Bode plots and is presented in the same table.

For the initial coating, the phase angle is 75° suggesting the existence on surface of a highly stable film, with a behavior close to pure capacitive impedance. The Nyquist diagram (Fig. 17 a) is a beginning of a semicircle with a large radius, and both the solution resistance and charge transfer resistance have high values. This proves that the thin PBG layer is a good insulator. The roughness factor is 0.84 because the surface is not perfectly flat, being mechanical polished and chemical etched before deposition in order to increase the surface active area and the bioactivity. CPE value was 1.46 nF which corresponds to a 400 nm thick of PBG film.

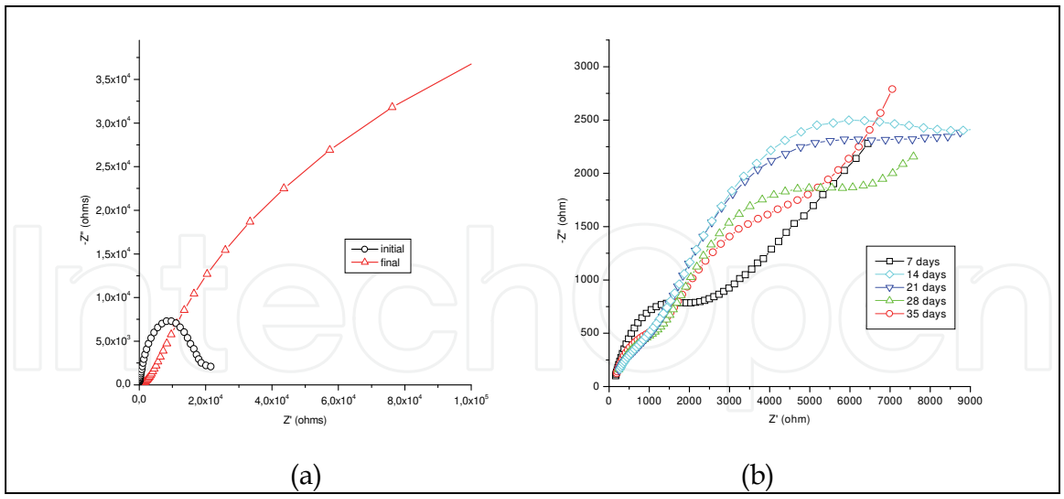

Fig. 17. Impedance spectra in complex plane for PBG61 sample: (a) initially, after 6 weeks immersion in SBF and b) after 1, 2, 3, 4, 5 weeks immersion in SBF at room temperature

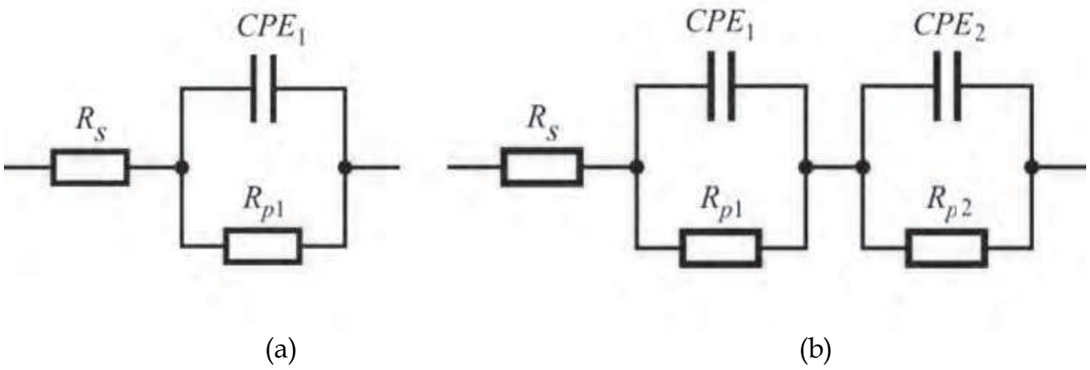

Fig. 18. Equivalent electrical circuits for PBG61 sample: (a) initially and after 6 weeks immersion in SBF and b) after 1, 2, 3, 4, 5 weeks immersion in SBF at room temperature

PBG61	R_s (Ω)	R_{p1} (kΩ)	CPE_1 10^{-6}(F)	n_1	φ_1 (°)	R_{p2} (kΩ)	CPE_2 10^{-6}(F)	n_2	φ_2 (°)
Initial	1111	18.44	0.00146	0.84	-75.0	-	-	-	-
1 week	103.8	15.36	2.10	0.82	-43.0	-	-	-	-
2 weeks	75.4	12.41	38.58	0.56	-43.0	0.48	12.02	0.58	-26.0
3 weeks	49.1	11.13	43.19	0.52	-43.0	0.87	8.76	0.58	-28.0
4 weeks	47.9	10.00	45.93	0.55	-42.0	0.90	8.03	0.65	-31.2
5 weeks	30.27	9.07	55.62	0.51	-42.0	1.125	2.88	0.67	-31.5
6 weeks	1799	-	-	-	-	$44 \cdot 10^4$	0.0072	0.95	-72.0

Table 5. Electrochemical impedance spectroscopy data of PBG61 sample after various immersion times in SBF at room temperature.

After immersion in SBF both the charge transfer resistance and solution resistance became smaller, the maximum phase angle decreased and another peak appeared in the Bode plot at 26° as an effect of the adsorption process (see Table 5). The BG dissolution leads to the flat surface degradation and the roughness factor gets much smaller. The Nyquist diagram (Fig. 17 b) shows two well defined time constants. These facts suggest that the two processes of the BG dissolution in SBF and the adsorption of some electrolyte ions on surface take place simultaneously causing the formation of a new liquid – layer interface. These results are in good agreement with experimental evidence obtained by FTIR and CLSM (Floroian, 2008; Sima, 2009) and support the formation on the metal surface of a new BHA phase, rather similar to the human bone composition.

The fitting of impedance spectra over the whole frequency range as generated the ($R_s[R_{p1}CPE_1]$ $[R_{p2}CPE_2]$) equivalent circuits with two parallel R-CPE elements in series (Fig. 18). The parallel group $[R_{p1}CPE_1]$ corresponds to an inner layer composed of PBG barrier layer while the parallel group $[R_{p2}CPE_2]$ corresponds to the outer layer consisting of the new forming BHA phase.

Large changes were found after every week of immersion in SBF (see Fig. 17 and Table 5). After 6 weeks the maximum phase angle reaches 72° and both the adsorption and diffusion processes were stopped. The charge transfer resistance and solution resistance were very high. The CPE value was 7.25 nF which corresponds to an ≈ 100 nm thick BHA film. Nyquist plot evidenced an almost intact coating, proving that the superficial BHA layer is coating the entire surface, completely shielding it against next fluid action. The roughness factor was now higher (0.95), suggesting that the BHA layer is compact. It has very high impedance and excellent corrosion properties. The metal ions release by corrosion or wear processes that may induce aseptic loosening after long term implantation into human body are thus avoided.

PBG57 and BGs samples exhibited a similar behavior with these PBG61 samples, except that the diffusion and adsorption processes disappeared after 5 weeks and after 2-3 weeks of immersion in SBF at room temperature, respectively. This means that the compact BHA layer was faster formed on these surfaces compared with PBG61 samples, when the BHA film appears after 6 weeks of immersion only. This delayed formation of the BHA film could be the effect of the increased bioactivity of BG57 samples in respect with PBG57 ones. PMMA addition has reduced the bone ability to bond to BG, but the advantage of using the composite PBG is that PMMA those not dissolved in SBF remaining on implant (Ti) surface. The BG bioactivity is however preserved and even enhanced by the formation of the new BHA phase on top surface of the layer (Floroian et al, 2010). As a consequence, the resistance Rp of PBG samples get higher values in the end and acts therefore as a better shield against corrosion of the Ti implant (substrate).

4.2.4 Influence of the working potential upon the PBG samples

The effect of the electrical potential applied upon the recorded EIS of the Ti coated samples (Fig. 19), was studied. In case of PBG61 samples well defined semicircles were recorded for all applied potentials. The increase of the semicircle diameter with the applied potential can be accounted for by the calcium and phosphorus ions adsorption from solution on sample surface. The adsorption blocked the electrode surface and rendered the charge transfer rather prohibitive. Consequently, the charge transfer resistance increased. A similar behavior was observed for other biological compounds when adsorbed on glassy carbon electrodes (Oliveira Brett, 2002, 2003; Brett, 1994).

In case of PBG57 samples similar semicircles were observed at +0.1 V, but largely differing ones at 0 V and particularly at -0.1 V. A purely capacitive behavior with constant phase angle characteristics were noticed at -0.1 V for the PBG57 sample. The shift of the angle downwards from 90° with respect to the real axis is due to the rather high value of the roughness factor of 0.8 - 0.85 (angle of ≈ 80°), as well as to the low curvature. This evolution is congruent with the existence of an almost intact coating. The formed superficial BHA layer has covered the entire surface thus completely isolating the Ti substrate. These studies demonstrated that the application of an electrical potential has accelerated the chemical processes between electrodes, leading to the formation in a matter of minutes of a compact continuous BHA layer. Thus, the higher activity of PBG57 sample in SBF was confirmed by the formation of the bioactive layer at -0.1 V. Conversely, in case of PBG61 sample, the BHA layer formation has not initiated at -0.2 V yet.
Finally, we advance the hypothesis that the faster repair of a fracture or the osteointegration could be achieved by the proper application of an electrical potential on hybrid PBG coatings covering Ti prostheses.

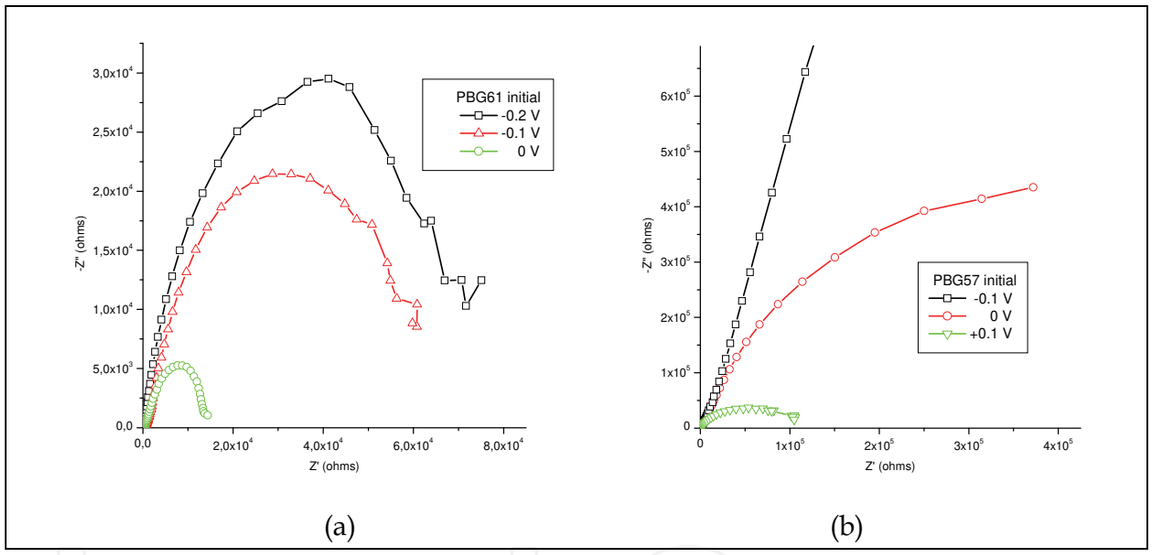

Fig. 19. EIS in the complex plane for PBG61 (a) and PBG57 (b) samples at different applied potentials in SBF at room temperature

5. Conclusions

An area of major interest in biomedical engineering is presently the development of new materials for medical implants. The bioactive glasses and glass ceramics have been extensively investigated in the past three decades for biomedical application due to their ability to form a tight bond to living bone.
Large research efforts have been directed to the new cations inclusion or mixture with biomaterials, thus providing novel properties to bioactive glasses. We reviewed in this chapter new results on the incorporation of the bioglass particles into a PMMA matrix in order to improve the mechanical and corrosion properties of bioglass coatings. The thin films of composite polymer-bioglass (PBG) were obtained by matrix assisted pulsed laser evaporation (MAPLE) - an advanced deposition technique which allows for the protected,

safe transfer of delicate substances sensible to damage under direct action of laser and plasma.

The biocompatibility and bioactivity of the composite films was evaluated in vitro, in two modes. First, the films transformation when immersed in SBF was evaluated by FTIR, CLSM and electrochemical studies. Next, biological tests have been performed using human osteoblasts cultured on films. One important evidence was the formation of a bioapatite layer by ions exchange with the fluid concurently with the bioglass decomposition. The polymer is not dissolved in SBF but is deposited on the surface. The electrochemical impedance spectroscopy studies demonstrated that as an effect of immersion in biological fluids, the implant corrosion is slowed down and the metal ions release in to the body is prohibited.

Human osteoblastes cultivated on the composite coatings that were immersed for several days in SBF remained very adherent to the substrate, exhibiting a very good viability and proliferation confirming the films biocompatibility and the stable fixation to bone.

The presence of the nanostructured PBG coatings on the metallic implants surface made the implant bioactive and more resistant to corrosion. The use of the MAPLE deposited nanocomposite PBG layers is suggested to be a promising alternative for development of a new generation of implants and prostheses.

6. Acknowledgment

A.P., N.S., and I.N.M. acknowledge we thanks the financial support of this work by the UEFISCSU (Romania) under the project IDEI, 511/ 2008.

7. References

Andersson, O. H.; Karlsson, K.H.; Kangasniemi, H. & Yli- Urpo, A. (1988). Models for physical properties and bioactivity of phosphate opal glasses. Glastechnische Berichte, Vol. 61, No.10, pp. 300-305, ISSN 0017-1085

Azevedo, M., Jell, G., Hill, R. & Stevens, M.M., (2008), Novel hypoxia mimicking bioactive materials for tissue engineering, Tissue Engineering Part A, Vol.14, No. 5, (May 2008), pp. 889 – 891, ISSN 1937-3368

Bliquez, LJ., (1996), Prosthetics in classical antiquity: Greek, Etruscan and Roman prosthetics. In: Aufstieg und niedergang der Römischen welt II, Haase W., Temporini H. (Eds.), pp. 2640-2676, Walter de Gruyter, ISBN 3-11-015714-4, Berlin & New York

Boccaccini, A.R., Erol, M., Stark, W.J., Mohn, D., Hong, Z. & Mano, J.F., (2010), Polymer/bioactive glass nanocomposites for biomedical applications: A review, Composites Science and Technology, Vol. 70, No. 13, (November 2010), pp. 1764 – 1776, ISBN 0266-3538

Bretcanu, O., Spriano, S., Vitale C.B. & Verne E., (2006), Synthesis and characterization of coprecipitation-derived ferrimagnetic glass–ceramic, Journal of Materials Science, Vol. 41, No. 4, (February 2006), pp. 1029 – 1037, ISSN 0022-2461

Brett, C. M. A.; Oliveira Brett, A. M. & Serrano, S. H. P. (1994).On the adsorption and electrochemical oxidation of DNA at glassy carbon electrodes. J Electroanal Chem, Vol.366, pp. 225-238, ISSN: 0022-0728

Brunner, T.J., Grass, R.N. & Stark, W.J, (2006), Glass and bioglass noanopowders by flame synthesis, Chemical Communications, Vol. 13, (2006), pp. 1384 – 1386, ISSN 1359-7345

Chan, C., Thompson, I., Robinson, P., Wilson, J. & Hench, L., (2002), Evaluation of Bioglass/dextran composite as a bone graft substitute, International Journal of Oral & Maxillofacial Surgery, Vol. 31, No. 1, (February 2002); pp. 73–77, ISSN 0901-5027

Chen, X., Lei, B., Wang, Y. & Zhao, N., (2009), Morphological control and in vitro bioactivity of nanoscale bioactive glasses, Journal Non- Crystalline Solids, Vol. 355, No. 13, (May 2009), pp. 791 – 796, ISSN 0022-3093

Couto, D.S., Hong, Z. & Mano, J.F., (2009), Development of bioactive and biodegradable chitosan-based injectable systems containing bioactive glass nanoparticles, Acta Biomaterialia, Vol. 5, No. 1, (January 2009), pp. 115 – 123, ISSN 1742-7061

Cristescu, R.; Mihailescu, I. N.; Jelinek, M. & Chrisey, D. B. (2006). Functionalized Thin Films & Structures Obtained by Novel Laser Processing Issues, In: Functionalized Properties of Nanostructured Materials, R. Kassing, P. Petkov, W. Kulisch & C. Popov (Eds.), 211-226, NATO Science Series by Springer, Series II: Mathematics, Physics and Chemistry, ISBN 1-4020-4595-6

Day, R.M., Boccaccini, A.R., Shurey, S., Roether, J.A., Forbes, A. & Hench, L.L., (2004), Assessment of polyglycolic acid mesh and bioactive glass for soft-tissue engineering scaffolds, Biomaterials, Vol. 25, No. 27, (December 2004), pp. 5857 – 5866, ISSN 0142-9612

Emsley, J., (2001), Nature's Building Blocks: An A-Z Guide to the Elements, Oxford University Press, ISBN 0-19-850340-7, Oxford, England, UK

Esfahani, S.I.R., Tavangarian, F. & Emadi, R., (2008), Nanostructured bioactive glass coating on porous hydroxyapatite scaffold for strength enhancement, Materials Letters, Vol. 62, No.19, (July 2008), pp. 3428 – 3430, ISSN 0167-577X

Floroian, L.; Savu, B.; Stanciu, G.; Popescu, A. C.; Sima, F.; Mihailescu, I. N.; Mustata, R.; Sima, L. E.; Petrescu, S. M.; Tanaskovic, D & Janackovic, D. J. (2008). Nanostructured bioglass thin films syntherized by pulsed laser deposition: CLSM, Ftir investigations and in vitro biotests. Appl. Surf. Sci. Vol.255, pp. 3056-3062, ISSN: 0169-4332

Floroian, L.; Sima, F.; Florescu, M. , Badea, M.; Popescu, A.C.; Serban, N. & Mihailescu, I.N. (2010). Double layered nanostructured composite coatings with bioactive silicate glass and polymethylmetacrylate for biomimetic implant applications. J Electroanal Chem, Vol.648, pp. 111-118, ISSN: 0022-0728

Floroian, L.; Mihailescu, I. N.; Sima, F.; Stanciu, G. & Savu, B. (2010) Evaluation of biocompatibility and bioactivity for pmma – bioactive glass nanocomposite films obtained by MAPLE. UPB Sci. Bull. Series A, Vol.72, Iss.2, pp. 133-148, ISSN: 1223-7027

Gomez-Vega, J. M.; Saiz, E. & Tomsia, A. P. (1999). Glass-based coatings for titanium implant alloys. J Biomed Mater Res., Vol.46, pp. 549-559, ISSN 0021-9304

Gomez-Vega, J.M, Saiz, E., Tomsia, A.P., Marshall, G.W. & Marshall, S.J. (2000), Bioactive glass coatings with hydroxyapatite and Bioglass ® particles on Ti-based implants, Biomaterials, Vol. 21, No. 2, (January 2000), pp. 105 – 111, ISSN 0142-9612

Gorustovich, A.A., Roether, J.A. & Boccaccini, A.R, (2010), Effect of bioactive glasses on angiogenesis: in-vitro and in-vivo evidence, Tissue Engineering Part B: Reviews, Vol. 16, (April 2010), pp.199–207, ISSN 1937-3368

Greenspan, D.C. & Hench, L .L., (1976), Chemical and mechanical behavior of bioglass-coated alumina, Journal of Biomedical Materials Research, Vol. 10, No. 4 (July 1976), pp. 503 – 509, ISSN 1549-3296

Gross, U.M. & Strunz V., (1980), The anchoring of glass ceramics of different solubility in the femur of the rat, Journal of Biomedical Materials Research, Vol. 14, No. 5, (September 1980), pp. 607 – 618, ISSN 1549-3296

Gyorgy, E.; Grigorescu, S.; Socol, G.; Mihailescu, I. N.; Figueras, A.; Janackovic D.; Palcevskis, E.; Zdrentu L. E. & Petrescu S. (2007). Bioactive glass and hydroxyapatite thin films obtained by pulsed laser deposition. Appl. Surf. Sci., Vol.19, pp. 7981 – 7986, ISSN: 0169-4332

Haimi, S., Gorianc, G., Moimas, L., Lindroos, B. & Huthala, H., (2009), Characterization of zinc-releasing three-dimensional bioactive glass scaffolds and their effect on human adipose stem cell proliferation and osteogenic differentiation, Acta Biomaterialia, Vol. 5, No. 8, (October 2009), pp.(3122 – 3231, ISSN 1742-7061

Hench, L.L., Clark, A.E., Schaake, J R. & Schaake H.F., (1972), Effects of microstructure on the radiation stability of amorphous semiconductors, Journal Non- Crystalline Solids, Vol. 8–10, (June 1972), pp. 837 – 843, ISSN 0022-3093

Hench, L.L. (1981), Fundamental Aspects of Biocompatibility, D. F.Williams (Ed), CRC Press, ISBN 0849366119, United States

Hench, L. L. (1991). Bioceramics: from concept to clinic. J. Am. Ceram.Soc., Vol.74, pp. 1487-1510, ISSN 0002-7820

Hench, L.L. & Wilson J., (October 1993), An Introduction to Bioceramics (Advanced Series in Bioceramics-vol. 1), World Scientific Publishing Company, ISBN 981-02-1400-6, Singapore

Hill R. (1996). An alternative view of the degradation of Bioglass. J Mater Sci Lett, Vol.15, pp. 1122-1125, ISSN 0261-8028

Hong, Z., Merino, E.G., Reis, R.L. & Mano, J.F., (2009), Novel Rice-shaped Bioactive Ceramic Nanoparticles, Advanced Engineering Materials, Vol.11, No. 15, (May 2009), pp. B25 –B29, ISSN 1438-1656

Karthega, M.; Tamilselvi, S. & Rajendran, N. (2008). Effect of pH on the corrosion behavior of Ti6Al4V alloy for dental implant application in fluoride media. Trends Biomater.Artif.Organs, Vol.20, No.1, pp. 31-39, ISSN 0971-1198

Kokubo, T.; Kushitani, H.; Sakka, S.; Kitsugi, T. & Yamamuro, T. (1990). Solutions able to reproduce in vivo surface-structure changes in bioactive glass-ceramic A-W3. J. Biomed. Mater. Res., Vol.24, pp. 721-734, ISSN 1549-3296

Lahav, A., Burks, RT., Greis, PE., Chapman, A.W., Ford, G.M. & Fink, B.P., (2006), Clinical outcomes following osteochondral autologous transplantation, Journal of Knee Surgery, Vol. 19, No. 3, (July 2006), pp. 169-173, ISSN 15388506

Lao, J., Nedelec, J.M. & Jallot, E. J., (2009), New strontium-based bioactive glasses: physicochemical reactivity and delivering capability of biologically active dissolution products, Journal of Materials Chemistry, Vol. 19, No. 19, (2009), pp. 2940 – 2949, ISSN 0959-9428

León, B. & Jansen, J., (2010), Thin Calcium Phosphate Coatings for Medical Implants, Springer, ISBN 978-0-387-77718-4, New York

Leu, A & Leach, J.K., (2008), Proangiogenic potential of a collagen/bioactive glass substrate, Pharmaceutical Research, Vol. 25, (May 2008), pp. 1222 – 1229, ISSN 0724-8741

Mihailescu, I. N.; Ristoscu, C.; Bigi A. & Mayer, I. (2010). Advanced biomimetic implants based on nanostructured coatings synthesized by pulsed laser technologies, In Laser-Surface Interactions for New Materials Production Tailoring Structure and Properties, A. Miotello & P.M. Ossi (Eds.), 235 – 260, Springer Series in Materials Science, ISSN: 0933-033X

Misra, S.K., Ohashi, F., Valappil, S.P., Knowles, J.C., Roy, I., Silva, S. R.P., Salih, V. & Boccaccini, A.R., (2010), Characterization of carbon nanotube (MWCNT) containing P(3HB)/bioactive glass composites for tissue engineering applications, Acta Biomaterialia, Vol. 6, No. 5, (March 2010), pp. 735 – 742, ISSN 1742-7061

Misra, S.K., Ansari, T.I., Valappil, S.P., Mohn, D., Philip, S.E., Stark, W.J., Roy, I., Knowles, J.C., Salih, V. & Boccaccini, A.R., (2010), Poly(3-hydroxybutyrate) multifunctional composite scaffolds for tissue engineering applications, Biomaterials, Vol. 31, No. 10, (April 2010), pp. 2806 – 2815, ISSN 0142-9612

Nelea, V.; Morosanu, C.; Iliescu, M. & Mihailescu, I.N. (2004). Hydroxyapatite thin films grown by pulsed laser deposition and radio-frequency magnetron sputtering: comparative study. Appl. Surf. Sci., Vol. 228, pp. 346–356, ISSN: 0169-4332

Ohura, K.; Nakamura, T.; Yamamuro, T.; Ebisawa, Y.; Kokubo, T.; Kotoura, Y. & Oka, M. (1992). Bioactivity of CaO SiO2 glasses added with various ions. J Mater Sci, Vol.3, pp. 95-100

Ogino, M.; Ohuchi, F. & Hench, L. L. (1980). Compositional dependence of the formation of calcium phosphate films on Bioglass. J Biomed Mater Res., Vol.14, pp. 55-64, ISSN 0021-9304

Oki, A, Parveen, B., Hossain, S., Adeniji, S. & Donahue, H, (2004), Preparation and in vitro bioactivity of zinc containing sol-gel–derived bioglass materials, Journal of Biomedical Materials Research A, Vol. 69A, No. 2, (May 2004), pp. 216 – 221, ISSN 1549-3296

Oliveira Brett, A. M.; Silva, L. A.; Farace, G.; Vadgama, P. & Brett, C. M. A. (2003). Voltammetric and impedance studies of inosine-5-monophosphate and hypoxanthine. Bioelectrochemistry, Vol.59, pp. 49-57, ISSN: 1567-5394

Oliveira Brett, A. M.; Silva L. A. & Brett, C. M. A. (2002). Adsorbtion of guanine, guanosine and adenine at electrodes studied by differential pulse voltammetry and electrochemical impedance. Langmuir, Vol.18, pp. 2326-2342

Oshida, Y., (2007), Bioscience and Bioengineering of Titanium Materials, Elsevier Science, ISBN 978-0-08-045142-8, Oxford

Park, J., (2008), Bioceramics: Properties, Characterizations, and Applications, Springer, ISBN 978-0-387-09544-8, New York

Perez, N. (2008). Electrochemistry and corrosion science. Norwell. USA: Kluwer Academic Publishers.

Pique, A. (2007). Deposition of Polymers and Biomaterials Using the Matrix-Assisted Pulsed Laser Evaporation (MAPLE) Process, In: Pulsed Laser Deposition of Thin Films: Applications-Led Growth of Functional Materials, R. Eason (Ed.), John Wiley & Sons, Inc., ISBN-13: 978-0-471-44709-2

Quintero, F., Mann, A.B., Pou, J., Lusquinos, F. & Riveiro, A., (2007), Rapid production of ultralong amorphous ceramic nanofibers by laser spinning, Applied Physics Letters, Vol. 90, No. 15, (March 2007) pp. 153109, ISSN 0003-6951

Quintero, F., Pou, J., Lusquinos, F. & Riveiro., A., (2007) Experimental analysis of the production of micro- and nanofibres by Laser Spinning, Applied Surface Science, Vol. 254, No. 4, (December 2007), pp. 1042 – 1047, ISSN 0169-4332

Quintero, F., Dieste, O., Pou, J., Lusquinos, F. & Riveiro, A., (2009), On the conditions to produce micro- and nanofibres by laser spinning, Journal of Physics D: Applied Physics, Vol. 42, No. 6, (March 2009), pp. 065501, ISSN 0022-3727

Quintero, F., Pou, J., Comesana, R., Lusquinos, F., Riveiro, A., Mann, A.B., Hill, R.G., Wu, Z.Y. & Jones, J.R., (2009), Laser Spinning of Bioactive Glass Nanofibers, Advanced Functional Materials, Vol. 19, No. 19, (August 2009) pp. 3084 – 3090, ISSN 1616-3028

Saiz, E.; Tomsia, A.P. & Pazo, A. (1998). Bioactive coatings on Ti and Ti6Al4V alloys for medical applications, In: Tomsia AP, Glaeser AM, (Eds), Ceramic microstructures: control at the atomic level, Berkeley, Plenum Press, pp. 543–550, ISBN 0-306-45817-9

Saiz, E.; Tomsia, A.P. & Pazo, A. (1998). Silicate glass coatings on Ti-based implants. Acta Mater, Vol.46, pp. 2551-2558, ISSN 1359-6454

Sepulveda, P., Jones, J.R., & Hench, L.L., (2001), Characterization of melt-derived 45S5 and sol-gel–derived 58S bioactive glasses, Journal of Biomedical Materials Research, Vol. 58, No. 6, (June 2001), pp. 734 – 740, ISSN 1549-3296

Sima, F.; Ristoscu, C. Popescu, A.; Mihailescu, I.N.; Kononenko, T.; Simon, S.; Radu, T.; Ponta, O.; Mustata, R.; Sima, L. E. & Petrescu, S. M. (2009). Bioglass -polymer thin coatings obtained by MAPLE for a new generation of implants. Journal of Optoelectronics and Advanced Materials, Vol.11, pp. 1170-1179, ISSN 1454-4164

Tanaskovic, D.; Jokic, B.; Socol, G.; Popescu, A.; Mihailescu, I. N.; Petrovic, R. & Janackovic D. (2007). Synthesis of functionally graded bioactive glass - apatite multistructures on Ti substrates by pulsed laser deposition. Appl. Surf. Sci. Vol.254, pp. 1279-1282, ISSN: 0169-4332

Tanaskovic, D.; Veljković, Dj.; Petrović, R.; Janaćković, Dj.; Mitrić, M.; Cojanu, C.; Ristoscu, C. & Mihailescu, I.N. (2008). Double layer bioactive glass coatings obtained by PLD. Key Engin. Mater. Vol.361-363, pp. 277-280, ISSN: 1013-9826

Vallet-Regi, M., Salinas, A.J., Roman, J. & Gil, M., (1999), Effect of magnesium content on the in vitro bioactivity of CaO-MgO-SiO2-P2O5 sol-gel glasses, Journal of Materials Chemistry, Vol. 9, No. 2, (1999), pp. 515 – 518, ISSN 0959-9428

Veljovic, Dj.; Jokic, B.; Petrovic, R.; Palcevskis, E.; Dindune, A.; Mihailescu, I. N. & Janackovic D. (2009). Processing of dense nanostructured HAP ceramics by sintering and hot pressing. Ceramics International, Vol.35, pp. 1407–1413, ISSN 0272-8842

Verrier, S., Blaker, J.J., Maquet, V. &Hench, L.L., (2004), PDLLA/Bioglass® composites for soft-tissue and hard-tissue engineering: an in vitro cell biology assessment, Biomaterials, Vol. 25, No. 15, (July 2004), pp. 3013 – 3021, ISSN 0142-9612

Vitale-Brovarone, C., Miola, M., Balagna, C. & Verne, E., (2008), 3D-glass-ceramic scaffolds with antibacterial properties for bone grafting, Chemical Engineering Journal, Vol. 137, No. 1, (March 2008), pp. 129 – 136, ISSN 1385-8947

Wheeler, D.L., Montfort, M.J. & McLoughlin, S.W., (2001), Differential healing response of bone adjacent to porous implants coated with hydroxyapatite and 45S5 bioactive glass, J Biomed Mat Res, Vol. 55, No. 4, (June 2001), pp. 603 – 612, ISSN 1549-3296

Xynos, I.D., Hukkanen, M.V.J., Batten J.J., Buttery L.D., Hench L.L. & Polak J.M., (2000), Bioglass ® 45S5 Stimulates Osteoblast Turnover and Enhances Bone Formation In Vitro: Implications and Applications for Bone Tissue Engineering, Calcified Tissue International, Vol. 67, No. 4, (March 2000), pp. 321-329, ISSN 0171-967X

Yao, J., Radin, S., Leboy, P.S. & Ducheyne, P., (2005), The effect of bioactive glass content on synthesis and bioactivity of composite poly (lactic-co-glycolic acid)/bioactive glass substrate for tissue engineering, Biomaterials, Vol. 26, No. 14, (May 2005), pp.1935 – 1943, ISSN 0142-9612

Zhang, K., Wang, Y., Hillmyer, M.A., Francis, L.F., (2004), Processing and properties of porous poly(Image -lactide)/bioactive glass composites, Biomaterials, Vol. 25, No. 13, (June 2004), pp. 2489–2500, ISSN 0142-9612

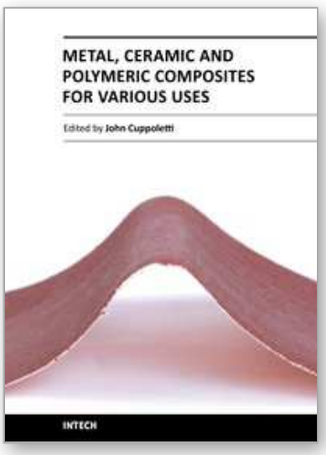

Metal, Ceramic and Polymeric Composites for Various Uses

Edited by Dr. John Cuppoletti

ISBN 978-953-307-353-8
Hard cover, 684 pages
Publisher InTech
Published online 20, July, 2011
Published in print edition July, 2011

Composite materials, often shortened to composites, are engineered or naturally occurring materials made from two or more constituent materials with significantly different physical or chemical properties which remain separate and distinct at the macroscopic or microscopic scale within the finished structure. The aim of this book is to provide comprehensive reference and text on composite materials and structures. This book will cover aspects of design, production, manufacturing, exploitation and maintenance of composite materials. The scope of the book covers scientific, technological and practical concepts concerning research, development and realization of composites.

How to reference

In order to correctly reference this scholarly work, feel free to copy and paste the following:

Laura Floroian, Andrei Popescu, Natalia Serban and Ion Mihailescu (2011). Polymer-Bioglass Composite Coatings: A Promising Alternative For Advanced Biomedical Implants, Metal, Ceramic and Polymeric Composites for Various Uses, Dr. John Cuppoletti (Ed.), ISBN: 978-953-307-353-8, InTech, Available from: http://www.intechopen.com/books/metal-ceramic-and-polymeric-composites-for-various-uses/polymer-bioglass-composite-coatings-a-promising-alternative-for-advanced-biomedical-implants

INTECH
open science | open minds

InTech Europe
University Campus STeP Ri
Slavka Krautzeka 83/A
51000 Rijeka, Croatia
Phone: +385 (51) 770 447
Fax: +385 (51) 686 166
www.intechopen.com

InTech China
Unit 405, Office Block, Hotel Equatorial Shanghai
No.65, Yan An Road (West), Shanghai, 200040, China
中国上海市延安西路65号上海国际贵都大饭店办公楼405单元
Phone: +86-21-62489820
Fax: +86-21-62489821

IntechOpen